Effect of diffusion and alloying on the magnetic and transport properties of Fe/V/Fe trilayers

Diana Iuşan
Institut de Physique et de Chimie des Matériaux de Strasbourg (IPCMS), UMR 7504 CNRS-ULP, 23 rue du Loess, 67034 Strasbourg, France
and Department of Physics, Uppsala University, Box 530, S-75112 Uppsala, Sweden

M. Alouani and O. Bengone
Institut de Physique et de Chimie des Matériaux de Strasbourg (IPCMS), UMR 7504 CNRS-ULP, 23 rue du Loess, 67034 Strasbourg, France

O. Eriksson
Department of Physics, Uppsala University, Box 530, S-75112 Uppsala, Sweden
(Received 30 October 2006; published 10 January 2007)

The magnetic and transport properties of the Fe/V/Fe(001) trilayers were studied using the self-consistent Green's function technique based on the tight-binding linear muffin-tin orbital method in the atomic-sphere approximation. The coherent potential approximation was used to describe the effects of interdiffusion and alloying at the interfaces on the properties of the semi-infinite bcc Fe(001)/*m*Fe/*n*V/*m*Fe/Fe(001) trilayers. The electric conductance was calculated using the Kubo-Landauer formalism, in the current-perpendicular-to-plane geometry. It is shown that a dipole moment is created at the Fe/V interface due to the charge transfer from vanadium to iron, and a small induced magnetic moment is present in the first vanadium layer and is antiparallel to that of iron. The interlayer exchange coupling shows rapid oscillations for small spacer thicknesses, and the interdiffusion and alloying at the interface stabilize the ferromagnetic coupling. Moreover, the interdiffusion reduces the vanadium-induced magnetic moment and increases the iron magnetic moment at the interface. The giant magnetoresistance (GMR) ratio presents damped oscillations as a function of the vanadium spacer thickness. The interdiffusion and the presence of Mn impurities at the interface reduce considerably the GMR ratio and produce results that are in agreement with experimental data.

DOI: 10.1103/PhysRevB.75.024412 PACS number(s): 71.20.Be, 71.15.Nc, 72.25.Mk

I. INTRODUCTION

The electronic structure and transport properties of Fe/V superlattices are the subject of intensive experiment and theoretical studies, due to the good epitaxy of the samples. In fact, experiments show that Fe/V superlattices can be grown epitaxially with little intermixing of iron and vanadium at the interfaces.[1,2] Broddefalk *et al.*[3] reported a good crystal quality of these samples, and a roughness of only about 2 monolayers (ML). It was noticed[4] that, although both bulk iron and vanadium have body-centered-cubic lattice structures, the lattice mismatch between iron and vanadium causes a symmetry breaking, and the superlattice becomes body-centered tetragonal (bct). The in-plane lattice parameter of the bct superlattice and the mean out-of-plane lattice parameter decrease with increasing iron layer thickness. Poulopoulos *et al.*[5] also revealed a good crystal quality and indicated a square symmetry in the plane of the film. It was also evidenced that the in-plane lattice parameter of the iron layers has increased, and that of the vanadium layers has decreased, compared to the corresponding bulk values. Due to the Poisson ratio, opposite changes occur for the out-of-plane lattice parameters.

It has been experimentally found that the Fe/V(001) superlattices exhibit oscillatory interlayer exchange coupling (IEC). In particular, the first evidence of an antiferromagnetic (AFM) IEC coupling in the Fe/V superlattices was given by Poulopoulos and co-workers[5] for the 13 ML thick vanadium spacer. A maximum of the AFM IEC was observed for about 6 ML of iron and 13 ML of vanadium,[4] and a corresponding giant magnetoresistance (GMR) ratio of 5% at low temperatures. These findings are also confirmed by Granberg *et al.*,[6] who found a GMR ratio of 7% at 10 K. However, it was noticed that the GMR effect observed for the Fe(3,6,9 ML)/V(13 ML) samples, disappears for 13Fe/13V.[4] The GMR and the AFM IEC vanish rapidly when increasing the iron thickness above 10 ML, and does not seem to reappear for larger thicknesses.[5,7] In other similar systems, as for example Fe/Cr (Ref. 8) or Fe/Ti,[9] the GMR remains finite for much larger thicknesses of the magnetic layer. Theoretically, the AFM coupling and its oscillations remain for relatively large magnetic layer thicknesses.[10] Granberg *et al.*[7] found a FM coupling between the magnetic slabs for the Fe(15 ML)/V(1–12 ML) systems. When iron is alloyed with Ni, as in the case of the $(Fe_{82}Ni_{18})$/V superlattices, the AFM IEC is shown to be weaker, and the GMR ratio decreases to 1.8%. A change from an AFM to a FM coupling can also occur, attributed to an increased interdiffusion between the FeNi and vanadium layers.

Concerning the coupling between the nearest-neighboring iron and vanadium layers, both experiment[11] and theory agree that it is an AFM one, and can be explained by hybridization effects.[12] However, differences occur when it comes to the values of the magnetic moments and the range of the spin polarization inside the vanadium spacer. While experimentally it is supposed to be of long-range magnetic order,

the theory predicts a shorter-ranged one. For example, Sacchi *et al.*[11] obtained experimental spin magnetic moments between $2.1\mu_B$ and $2.3\mu_B$ per iron atom and a total magnetic moment of $0.66\mu_B$ per vanadium atom in the 1 ML vanadium sample. They also observed that, with respect to the values for the 1 ML vanadium sample, the magnetic moment per vanadium atom is reduced to 60% and 40% in the case of the 2 ML and 5 ML samples, respectively. Schwickert and co-workers[13] found very large magnetic moments, but their results were confirmed neither by other experiments nor by theoretical calculations. A possible explanation to these differences may be found in the theoretical work of Holmström *et al.*, who showed that the interdiffusion and roughness between the iron and vanadium layers bring the calculated relevant magnetic properties in agreement with the experiment results.[14]

The aim of this paper is to present an *ab initio* study of the magnetic and transport properties of the *m*Fe/*n*V/*m*Fe trilayers sandwiched between two semi-infinite bcc iron leads, in the current-perpendicular-plane (CPP) geometry, and to study the changes of these properties by atomic intermixing at the interfaces. The effect of alloying with 3*d* transition metals at the interfaces using the coherent potential approximation[15] (CPA) will also be presented.

The rest of the paper is organized as follows. In the next section, we provide some details concerning the method of calculations. In the third section we discuss the electronic and magnetic properties of the ideal trilayer system as well as the IEC as a function of the spacer thickness and interdiffusion concentration. In the fourth section we present our results of the calculated GMR for the ideal trilayers and show the dominant channel for transport. We also show the effect of interdiffusion and impurities on the conductance.

II. METHOD OF CALCULATION

The electronic structure of Fe/V/Fe trilayers was determined using a first-principles Green's function technique[16,17] based on the tight-binding linear muffin-tin orbital method[15] in the atomic-sphere approximation.[18,19] The space-filling atomic spheres are chosen to be the same for both iron and vanadium atoms. The local spin density approximation was used for the exchange-correlation potential within the Vosko-Wilk-Nusair parametrization.[20]

The transport properties were calculated by means of the Kubo-Landauer formalism, where the conductance G^σ for spin σ can be expressed as[21]

$$G^\sigma = \frac{e^2}{h}\frac{1}{N_\parallel}\sum_{\mathbf{k}_\parallel}\int dE\left(-\frac{d}{dE}f(E)\right)T^\sigma(\mathbf{k}_\parallel,\mathbf{E}), \qquad (1)$$

where $f(E)$ is the equilibrium Fermi-Dirac distribution function and $T^\sigma(\mathbf{k}_\parallel,\mathbf{E})$ is the transmission probability for channel $(\mathbf{k}_\parallel,\sigma)$ at energy E and for each channel $\mathbf{k}_\parallel$ of the surface Brillouin zone (SBZ).[22] In the case of diffused interfaces or for impurity calculations, the CPA potential parameters, obtained from a self-consistent electronic structure calculation, are used for the electric transport, and the disorder is approximated by two-dimensional supercells with random occupation of lattice sites by two kinds of atoms. Their ratio corresponds to the concentration of the atoms in a given layer. We have found that the use of 4×4 two-dimensional lateral supercells and averaging the conductances over ten configurations provides the same results as the use of the CPA approach by evaluating the vertex correction as demonstrated by Carva and co-workers.[23] Our 3*d* transition metal impurities are all performed using the CPA vertex correction.

For the self-consistent band structure calculations the convergence was obtained for using 1000 **k** points in the irreducible SBZ, and 400 **k** points in the 4×4 supercell SBZ for the calculation of the conductances including the effect of diffusion.

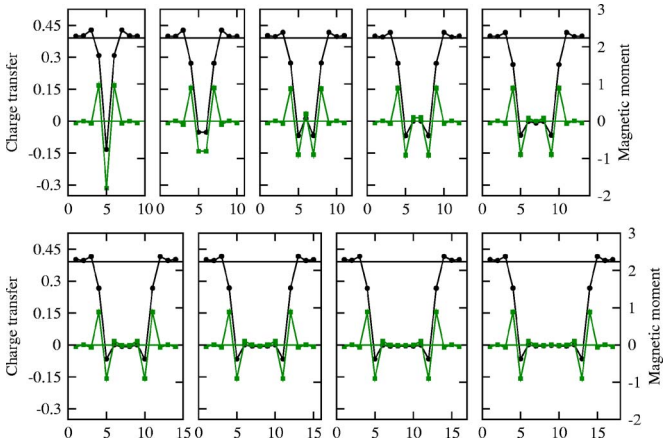

FIG. 1. (Color online) The variation of the magnetic moment (black circles) and the charge transfer (green squares) versus the layer index for Fe(001)/*n*V/Fe(001) systems with $n=1-9$ for the FM configuration. Four iron layers are taken into account on each side of the vanadium slab in the active region, embedded in semi-infinite bcc (001) bulk iron. The horizontal lines correspond to the bulk magnetic moment and charge transfer, introduced for comparison. The connecting lines are guides to the eye.

III. MAGNETIC PROPERTIES

A. Ideal trilayers

Figure 1 shows the variation of the magnetic moment and charge transfer at the interface for different spacer thicknesses. We observe important differences occurring at the interface layers as compared to the bulk electronic structure and smaller changes on the second layer from the interface. For the rest of the layers, the variations of the charge and the spin moments, are insignificant. At the interface the charge transfer is from vanadium to iron, which is consistent with the electronegativity of these elements. We note, however, that the determination of charge transfer in itinerant systems is difficult, and in our case, it depends to some extent on the choice of atomic-sphere radii.

The electronic structure calculations reveal a strong hybridization at the interface, mainly between vanadium and iron for the minority-spin channel. This decreases the magnetic moment of iron for the interface and induces a negative spin polarization on the vanadium atoms. As a consequence the vanadium atom at the interface is AFM coupled to the

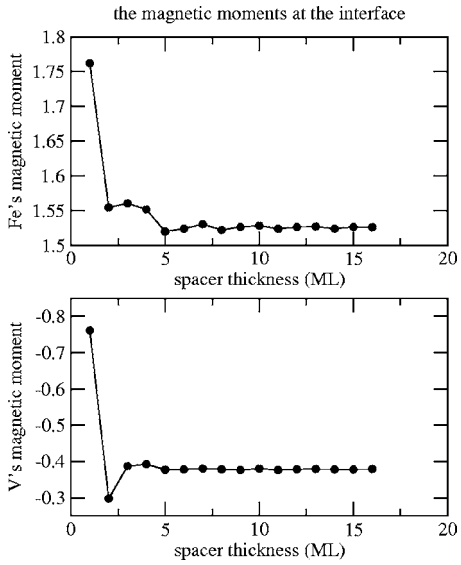

FIG. 2. The dependence of the interface moments of iron (upper panel) and vanadium (lower panel) as a function of the spacer thickness in the FM configuration of Fe/nV/Fe.

iron atoms, independently of the thickness of the spacer or the configuration of the magnetic slabs. It is also important to observe the short-ranged spin polarization of the vanadium atoms, confirmed by the dependence of the vanadium's interface magnetic moment as a function of the spacer thickness. This short-ranged spin polarization is in agreement with all previous theoretical results. A recent x-ray magnetic circular dichroism experimental study[24] confirms the short-range spin polarization of the Fe/V superlattices grown at low temperatures (300 K), where a small interdiffusion at the interfaces is expected. It was also found that the spin polarization becomes long ranged for superlattices grown at higher temperatures (600 K). However, theoretical calculations do not confirm this trend in the case of interdiffused interfaces. This discrepancy could be due to the fact that interdiffusion is supposed to extend only to two interface layers. Despite the small roughness in Fe/V superlattices, the interdiffusion between the iron and vanadium slabs could extend to more than 1–2 ML, as was assumed until now in *ab initio* calculations.

Figure 2 shows that the magnetic moments for both iron and vanadium are largest for $n=1$. The reason for this is that, in this case, each vanadium atom has eight nearest iron neighbors; a large hybridization between vanadium 3d and iron 3d states takes place. According to Ref. 12 this causes a large induced vanadium moment. For $n \geq 2$ each vanadium atom at the interface has only four nearest neighbors, which reduces the induced moment. One observes also a tendency of oscillatory behavior of the iron magnetic moment as a function of n. A "saturation" of the induced polarization for vanadium is observed. This confirms that the magnetic order of vanadium is concentrated at the interface, and is caused by a direct hybridization between vanadium and iron atoms. In addition, the vanadium next-nearest neighbors seem to have almost no influence upon the vanadium interface moment, due to the fact that their magnetic moments are small.

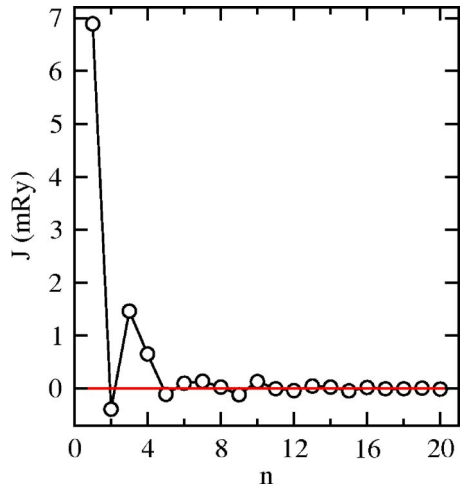

FIG. 3. (Color online) The dependence of the interlayer exchange coupling J in mRy as a function of the number of spacer layers n for the Fe/nV/Fe systems.

The IEC has been calculated as the energy difference of the systems with antiferromagnetically and ferromagnetically coupled magnetic slabs. Figure 3 shows the dependence of the IEC on the spacer thickness n. We notice a strong FM coupling for $n=1$, followed by an oscillatory behavior, with an amplitude that decreases very fast as the spacer thickness increases. Granberg *et al.*[7] studied the 15Fe/(1–12)V superlattices but did not find any sign of AFM coupling. We believe that this is due to the large thickness of the magnetic slabs used in their experiment, as it has been experimentally shown[4] that the IEC drops considerably for large slab thicknesses, as is confirmed by our calculations. Experimental studies[4,5] performed on Fe/V superlattices found a maximum in the AF IEC for a spacer thicknesses of about 13 ML. It is also seen that for $n \geq 16$ the IEC has approximately a zero value. A decrease of the IEC for large spacer thicknesses has been experimentally observed.[4]

B. Effect of interdiffusion

Figure 4 shows the dependence of the magnetic moments at the interface as a function of the interdiffusion concentra-

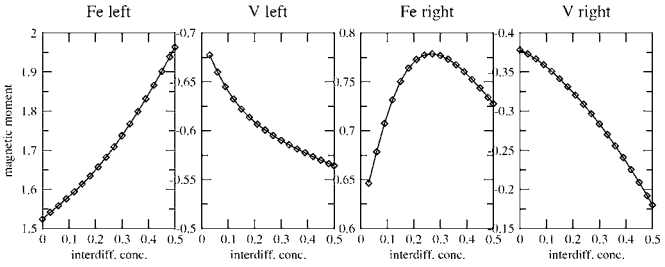

FIG. 4. The interface magnetic moments as a function of the interdiffusion concentration in the FM configuration of Fe/$Fe_{1-x}V_x$/Fe_xV_{1-x}/V. "Fe left" denotes iron atoms in the left interdiffused region and "vanadium left" denotes vanadium atoms in the same region. The "iron right" and "vanadium right" denote atoms in the right interdiffused region.

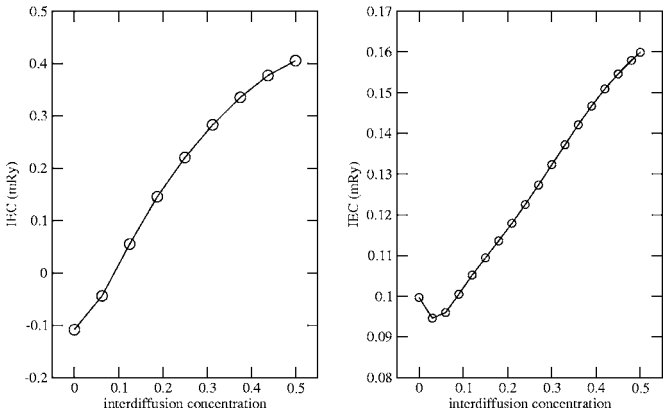

FIG. 5. The IEC as a function of the interdiffusion concentration for the Fe/5V/Fe (left side figure) and Fe/6V/Fe (right side figure) trilayers.

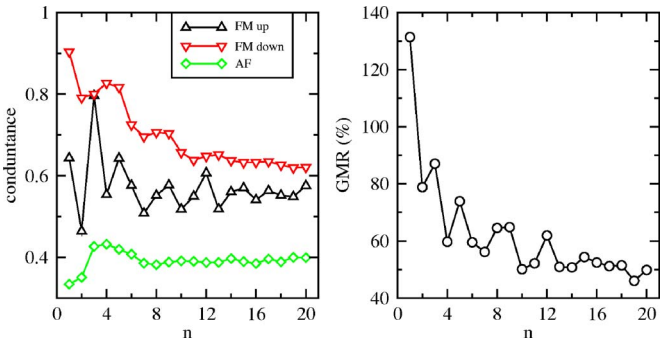

FIG. 6. (Color online) The conductances (left) and the GMR (right) as a function of the spacer thickness. The conductance for up spins is in black up triangles, that for down spins in red down triangles, and that of the AFM configuration in green diamonds. The continuous lines are guides to the eye.

tion x in the case of FM coupling between the magnetic slabs. The same variations are observed in the AFM case. Due to the geometry of the interdiffused interface, it becomes relevant to discuss vanadium atoms in the right side of the Fe/V interface, and vanadium atoms to the left of the interface. The latter atoms have interdiffused into what nominally is the iron side of the interface, and a small alloy region is formed.

The magnitude of the vanadium magnetic moment at the right side of the interface decreases as x increases due to the decrease of the number of iron nearest neighbors. The opposite happens for iron at the left of the interface due to the decrease of vanadium nearest neighbors and at the same time the increase of iron nearest neighbors. The size of the vanadium moment at the left of the interface decreases as a function of x although the number of iron nearest neighbors increases. This is probably due to the magnetic frustration caused by the FM coupling with the vanadium atoms surrounding it. A peculiar dependence is found for the iron magnetic moment of the atoms at the right interface; at first the moment increases and after reaching a maximum it decreases.

The dependence of the IEC for the Fe/nV/Fe systems ($n=5,6$), calculated as the difference between the energy in the AFM configuration and the energy in the FM configuration, is shown in Fig. 5. We observe that the IEC increases almost linearly as a function of the concentration. It is especially interesting that for $n=5$ the IEC changes sign, i.e., the coupling starts out being AFM but the interdiffusion at the interface favors the FM coupling and causes a phase transition from AFM to FM coupling for an interdiffusion concentration of $\sim 10\%$.[25]

IV. TRANSPORT PROPERTIES

A. Ideal trilayers

Figure 6 shows the spin-resolved conductance and the GMR as a function of spacer thickness. The oscillations of the GMR ratio as a function of the spacer thickness are seen to be due, mainly, to the oscillations of the conductance in the FM configuration. A period of about 4 ML is found for the conductance for spin up, but the oscillations seem to attenuate as n increases. This behavior was also obtained for Fe(110)/V/Fe(110) trilayers.[26] The conductance for the spin-down channel also presents oscillations, which attenuate more rapidly (for $n \geq 12$). The conductance in the antiparallel configuration presents a very small value for $n=1,2$, then it increases and decreases again slowly, and for $n \geq 7$ it is showing almost no variation. Therefore, the oscillations of the GMR are due to oscillations of the conductance in the FM case, especially in the spin-up channel, and the decrease in GMR as n increases is primarily due to the conductance of the two spin channels for the spin-down channel (in the FM configuration).

As compared to other systems (Fe/Cu, for example) the conductance of the two spin channels do not differ very much. Also, in the FM configuration the conductance for spin-down states is greater than for spin-up states. To explain this behavior we have shown in Fig. 7 the **k**-space-resolved density of states at the Fermi level for the interface layers of iron and vanadium and for the two spins which represent the spin-polarized two-dimensional Fermi surface at the interface. It is clear from this figure that the Fermi surface of the vanadium layer and that of iron resemble each other more for spin-down states than for spin up. In particular, the ring surrounding the Γ point of the SBZ are almost identical. Thus, the matching of these energy levels at the Fermi surface leads to an increased conductance for this channel as shown in the **k**-space-resolved conductance for both spins given in Fig. 8. The Fermi surface can also explain why the conductance in the AFM is even lower, as expected for a system with a positive GMR.

B. Effect of interdiffusion

Figure 9 shows the effect that interdiffusion at the interface has on the GMR of the Fe/5V/Fe and Fe/6V/Fe systems. The intermixing has a great effect on the conductance in the AFM configuration, and its conductance determines the behavior of the GMR as a function of the interdiffusion concentration x. The interdiffusion reduces the GMR very

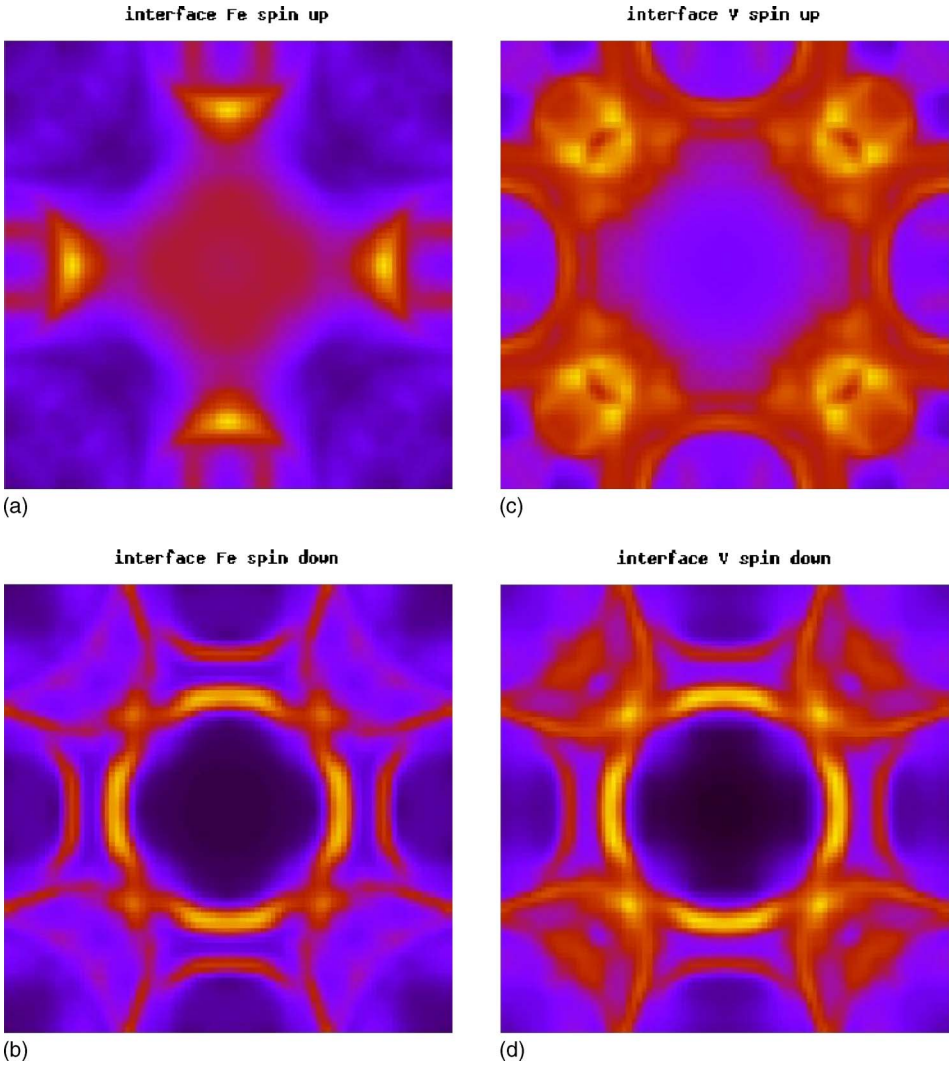

FIG. 7. (Color online) The upper left and right panels represent, respectively, the calculated density of states at the Fermi level for spin-up and spin-down states of iron at the interface. The lower left and right panels represent those of vanadium at the interface. The red color (light gray) represents the highest density of states at the Fermi level and the blue (dark gray) the lowest.

drastically. For example, for an interdiffusion concentration of only 20%, the GMR ratio is more than halved. We also observe a "saturation" of the GMR as x is increased. A value of 7% of the GMR for the 3Fe/13V superlattice was reported experimentally,[6] which is smaller than our calculated saturated value of $\sim 20-30$ %. The difference could be attributable to several causes: (a) the theoretical calculations correspond to spacer thicknesses of 5–6 ML, while the experiments to a spacer thickness of 13 ML; (b) the value of 50% is for the ideal system, and a great decrease is expected by allowing interdiffusion at the interfaces (because although a good interface roughness for the Fe/V superlattice was found, one cannot ignore the interdiffusion which exists in every real system); (c) the value is obtained for a trilayer system, while the experimental value is for superlattices with many repetitions, and, as was theoretically shown, a decrease of the GMR ratio appears as the number of repetitions increases; (d) the calculations were performed for the CPP geometry, whereas the experiment measures are in the current-in-plane geometry, and it is believed that the values of the GMR ratio are higher in the CPP geometry.

C. Effect of alloying at the interfaces

In this section we present the effect of impurities at the interfaces. This effect on the transport properties of Fe/V/Fe trilayers can be only indicative, because we have considered only the impurities in a single layer at both interfaces. A more realistic calculation of alloying would have to extend the impurities over many layers. However, such calculations are very time consuming, and have not been treated. As stated in Sec. II, the self-consistent potential is determined using the coherent potential approximation, for systems where $3d$ transition metal impurities are randomly distributed, either in the vanadium layer or in the iron layer at both interfaces. For the transport calculations, we have checked that the averaged conductance over ten alloy configurations in a 4×4 two-dimensional lateral supercell produced the same results as these of the effective medium CPA with vertex corrections.[23] The conductance is therefore calculated using the latter method. The Ti or Cr impurities are randomly distributed on the vanadium layer at both interfaces, corresponding to layer alloy composition of $V_{1-x}Ti_x$ or $V_{1-x}Cr_x$. The trilayer system is then described by $5Fe/V_{1-x}M_x/11V/V_{1-x}M_x/5Fe$, where M=Ti or Cr. The Mn or Co impu-

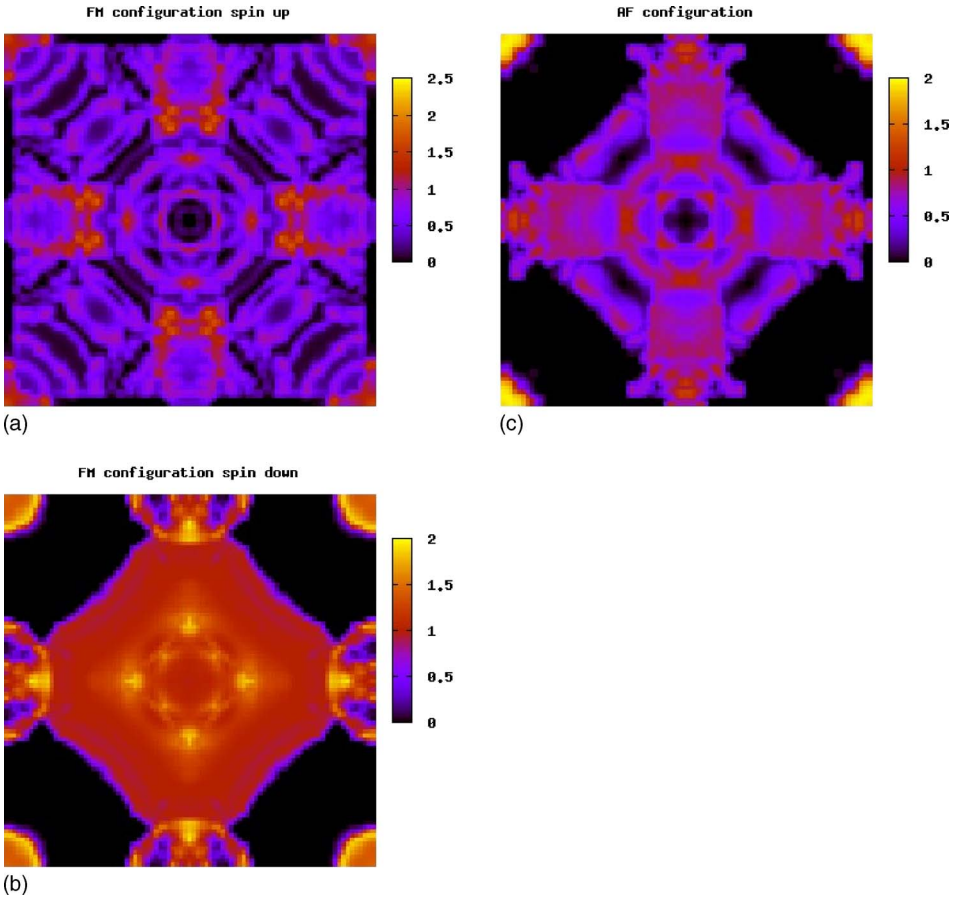

FIG. 8. (Color online) **k**-space-resolved conductance for spin-up and spin-down states in the FM configuration (left panel and middle panel, respectively), and antiferromagnetic configuration (right panel). The red color (light gray) represents the highest conductance and the blue (dark gray) the lowest.

rities are randomly distributed on the iron layer at both interfaces, corresponding to layer alloy composition of $Fe_{1-x}Mn_x$ or $Fe_{1-x}Co_x$. The trilayer system is then described by $4Fe/Fe_{1-x}M_x/13V/Fe_{1-x}M_x/4Fe$,where M=Mn or Co.

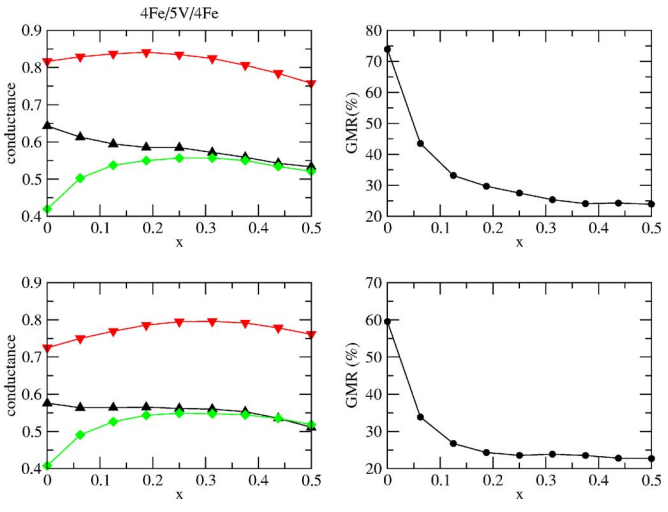

FIG. 9. (Color online) The conductances (left) and the GMR (right) as a function of the interdiffusion concentration for the Fe/5V/Fe (the top graphs) and Fe/6V/Fe systems (the bottom graphs). The red down triangles represent the spin-down conductance, the up black ones the spin-up conductance, and the green diamond the antiferromagnetic conductance. The continuous lines are guides to the eye.

The case where the impurities are put on both the vanadium and the iron layers at the interface will be of great interest, but are not performed in this study.

Figure 10 shows the dependence of the giant magnetoresistance on the concentration of impurities at the interface. In the case of chromium impurities, the GMR is almost inde-

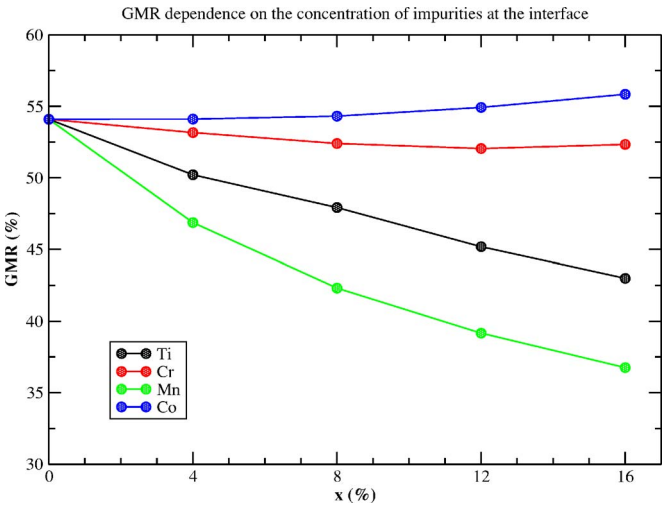

FIG. 10. (Color online) The GMR dependence on the concentration of the 3*d* transition metal impurities at the interfaces. The upper blue curve, the second from the top (red curve), the third (black curve), and the lowest curve represent, respectively, the case of Co, Cr, Ti, and Mn impurities.

pendent of the concentration of impurities. This is due to the good matching of the iron and chromium bands for the minority spin. Note, however, that in the case of Co/V/Co trilayers, the effect of chromium was important and was at the origin of negative giant magnetoresistance.[27] In case of Ti and Mn impurities, the GMR shows a rapid decrease with increasing concentration. Interestingly, the cobalt impurities at the interface increase the GMR by a small amount.

V. CONCLUSIONS

We have performed *ab initio* calculations of the magnetic and transport properties with or without the effect of interdiffusion and alloying at the interface of the Fe/V/Fe trilayers. The values of the magnetic moments are in good agreement with the experimental ones, when the effect of alloying is taken into account. This fact was also noted in Ref. 14 In the case of the ideal interface without diffusion, we obtained oscillations of both the IEC and GMR ratio. In the case of interdiffusion and alloying at the interface, we have obtained a considerable drop of the GMR as the interdiffusion concentration (or the impurity concentration) increases. This evidences the important role played by the interface in the case of the Fe/V/Fe systems. We have also shown that the GMR effect can be heavily dependent on the concentration of impurities at the interface, e.g., Mn and Ti impurities.

ACKNOWLEDGMENTS

We would like to thank CINES for providing us with supercomputer time (Project No. gem1100). O.E. acknowledges support from the Swedish Research Council and SSF. M.A. and O.B. acknowledge support from the French ANR p-nano.

[1] P. Isberg, B. Hjörvarsson, R. Wäppling, E. B. Svedberg, and L. Hultman, Vacuum **48**, 483 (1997).
[2] G. Andersson, B. Hjörvarsson, and P. Isberg, Phys. Rev. B **55**, 1774 (1997).
[3] A. Broddefalk, P. Nordblad, P. Blomquist, P. Isberg, R. Wäppling, O. Le Bacq, and O. Eriksson, J. Magn. Magn. Mater. **241**, 260 (2002).
[4] A. Broddefalk, R. Mathieu, P. Nordblad, P. Blomqvist, R. Wappling, J. Lu, and E. Olsson, Phys. Rev. B **65**, 214430 (2002).
[5] P. Poulopoulos, P. Isberg, W. Platow, W. Wisny, M. Farle, B. Hjörvarsson, and K. Baberschke, J. Magn. Magn. Mater. **170**, 57 (1997).
[6] P. Granberg, P. Isberg, E. B. Svedberg, B. Hjörvarsson, P. Nordblad, and R. Wäppling, J. Magn. Magn. Mater. **186**, 154 (1998).
[7] P. Granberg, P. Nordblad, P. Isberg, B. Hjörvarsson, and R. Wäppling, Phys. Rev. B **54**, 1199 (1996).
[8] R. Schad, C. D. Potter, P. Belliën, G. Verbank, V. V. Moshchalkov, and Y. Bruynseraede, Appl. Phys. Lett. **64**, 3500 (1994).
[9] T. Stobiecki, M. Czapkiewicz, M. Kopcewicz, R. Źuberek, and F. J. Castano, Thin Solid Films **317**, 306 (1998).
[10] S. K. J. Lenczowski, M. A. M. Gijs, J. B. Giesbers, R. J. M. van de Veerdonk, and W. J. M. de Jonge, Phys. Rev. B **50**, 9982 (1994).
[11] M. Sacchi, A. Mirone, C. F. Hague, J. M. Mariot, L. Pasquali, P. Isberg, E. M. Gullikson, and J. H. Underwood, Phys. Rev. B **60**, R12569 (1999).
[12] B. Szpunar and K. Kozarzewski, Phys. Status Solidi B **82**, 205 (1977).
[13] M. M. Schwickert, R. Coehoorn, M. A. Tomaz, E. Mayo, D. Lederman, W. L. O'Brien, T. Lin, and G. R. Harp, Phys. Rev. B **57**, 13681 (1998).
[14] E. Holmström, L. Nordström, L. Bergqvist, B. Skubic, B. Hjörvarsson, I. A. Abrikosov, P. Svedlindh, and O. Eriksson, Proc. Natl. Acad. Sci. U.S.A. **101**, 4742 (2004).
[15] I. Turek, V. Drchal, J. Kudrnovský, M. Sob, and P. Weinberger, *Electronic Structure of Disordered Alloys, Surfaces and Interfaces* (Kluwer, Boston, 1997).
[16] H. L. Skriver and N. M. Rosengaard, Phys. Rev. B **43**, 9538 (1991).
[17] H. L. Skriver and N. M. Rosengaard, Phys. Rev. B **46**, 7157 (1992).
[18] O. K. Andersen and O. Jepsen, Phys. Rev. Lett. **53**, 2571 (1984).
[19] O. K. Andersen, Z. Pawlowska, and O. Jepsen, Phys. Rev. B **34**, 5253 (1986).
[20] Vosko, Can. J. Phys. **58**, 1200 (1980).
[21] S. Datta, *Electronic Transport in Mesoscopic Systems* (Cambridge University Press, Cambridge, U.K., 1995).
[22] J. Kudrnovský, V. Drchal, C. Blaas, P. Weinberger, I. Turek, and P. Bruno, Phys. Rev. B **62**, 15084 (2000).
[23] K. Carva, I. Turek, J. Kudrnovský, and O. Bengone, Phys. Rev. B **73**, 144421 (2006).
[24] A. Scherz, P. Poulopoulos, R. Nünthel, J. Lindner, H. Wende, F. Wilhelm, and K. Baberschke, Phys. Rev. B **68**, 140401(R) (2003).
[25] B. Skubic, E. Holmström, D. Iuşan, O. Bengone, O. Eriksson, R. Brucas, B. Hjörvarsson, V. Sanciu, and P. Nordblad, Phys. Rev. Lett. **96**, 057205 (2006).
[26] R. C. Herper, L. Szunyogh, and P. Entel, Phys. Status Solidi B **242**, 272 (2005).
[27] O. Bengone, O. Eriksson, S. Mirbt, I. Turek, J. Kudrnovský, and V. Drchal, Phys. Rev. B **69**, 092406 (2004).